Available online at www.sciencedirect.com

ScienceDirect

Natural Gas Industry B 3 (2016) 45–51

www.elsevier.com/locate/ngib

Research article

Breakthrough in staged fracturing technology for deep shale gas reservoirs in SE Sichuan Basin and its implications☆

Zeng Yijin, Chen Zuo, Bian Xiaobing*

Sinopec Research Institute of Petroleum Engineering, Beijing 100101, China

Received 11 September 2015; accepted 10 February 2016
Available online 2 July 2016

Abstract

In the Southeastern Sichuan Basin, the deep shale reservoirs (with vertical depth over 2800 m) are complicated and diverse in reservoir mineral compositions and pore structural characteristics, with the obvious rock plasticity and nonlinear fracturing features and the high absolute difference between maximum and minimum principal stresses, due to the effect of geological setting and diagenesis. Consequently, staged fracturing operations often suffer from high fracturing pressure and propagating pressure, small fracture width, low sand–fluid ratio and fracture conductivity and difficult formation of volume fractures, which seriously influence the post-fracturing shale gas productivity. In this paper, a new combined fracturing mode (pretreatment acid + gelled fluid + slickwater + gelled fluid) and its supporting technologies were developed after a series of analysis and studies on deep rocks in terms of mechanical property, earth stress characteristics, fracturing characteristics and fracture morphology characteristics. Field application shows that geologic breakthrough was realized in Longmaxi Fm of Lower Silurian in Well Dingye 2HF, with absolute open flow (AOF) of 10.5×10^4 m^3/d after fracturing. And it was expected to reach commercial breakthrough in Qiongzhusi Fm of Lower Cambrian in Well Jinye 1HF, with AOF of 10.5×10^4 m^3/d after fracturing. Finally, the following conclusions are reached. First, it is hard to form complex fractures in deep shale and the fracturing technologies applicable for it should be different from those used in mid–deep zones. Second, the established fracturing pressure model can provide an effective way for deep-zone fracturing pressure prediction. Third, reducing operation pressure is one of the key measures to ensure successful deep-zone fracturing. Fourth, besides good material basis, it is crucial to increase the complexity of induced fractures and generate high-conductivity fractures in order to guarantee successful fracturing in deep shale.

Keywords: SE Sichuan Basin; Shale gas; Deep zone; Nonlinear deformation; Fracturing pressure; High flow conductivity; Staged fracturing; Application effects

Thanks to a large amount of technical and capital investments in recent years, medium-deep and deep shales in Jiaoshiba and Weiyuan–Changning have yielded commercial gas flow from the Silurian Longmaxi Fm through horizontal well drilling and fracturing; it is planned to realize a productivity of 50×10^8 m^3 in 2015. Some prospects, e.g. deep Jiaoshiba, Dingshan and Jingyan–Qianwei ($H_{vertical} > 2800$ m), have been discovered with pervasive shale gas accumulation with a large volume of resources; but shale gas production faces several challenges in multi-stage fracturing resulting from the variation of reservoir burial depth, temperature and earth stress [1–6]. (1) Rock brittleness, plasticity and fracturing behavior change greatly due to the variation of mineral composition, burial depth and formation temperature. It is hard to predict the increased fracturing pressure. (2) Narrowed fracture width due to the increase of the minimum principal stress makes it difficult to improve proppant–fluid ratio and proppant volume and construct the fractures with sustained high flow conductivity. (3) It is hard to achieve fracture network and volumetric stimulation due to the

☆ Project supported by Sinopec Science and Technology Project "Optimized stimulation of shale gas zones in Fuling block" (Grant No. P14091).
* Corresponding author.
E-mail address: xiaobingbian@126.com (Bian XB.).
Peer review under responsibility of Sichuan Petroleum Administration.

http://dx.doi.org/10.1016/j.ngib.2016.02.005

large absolute difference between the maximum and minimum principal stresses, limited operating distance of induced stress and deteriorated brittleness. Therefore, a successful deep shale fracturing is closely related to the safe fracturing under high pressure to establish a complicated fracture network with sustained high flow conductivity.

In this paper, a model was built to predict the fracturing pressure of shale with non-linear deformation based on the understanding of characteristic parameters of deep shale fracturing and a new fracturing method with "pretreatment acid + gelled fluid + slick water + gelled fluid" was proposed to lower operating pressure and improve proppant−fluid ratio, flow conductivity and stimulated volume of reservoir. Three wells were included in the field test. Well Dingye 2HF yielded shale gas of 10.5 × 10^4 m^3/d from Lower Silurian Longmaxi Fm after fracturing. Well Jinye 1HF achieved shale gas open flow (AOF) of 10.5 × 10^4 m^3/d from Lower Cambrian Qiongzhusi Fm after fracturing; as per stable post-frac output in the production testing, it is anticipated that this well may yield commercial gas flow. Through the field test, understanding on fracturing techniques for deep shale gas production was deepened.

1. Deep shale fracturing behavior in SE Sichuan Basin

Dingye 2HF, Nanye 1HF and Jinye 1HF are three horizontal gas wells in Dingshan, Nanchuan and Jingyanqianwei prospects, respectively, in SE Sichuan Basin. The zones of interest are Lower Silurian Longmaxi Fm and Lower Cambrian Qiongzhusi Fm with large burial depths (TVD of 4417 m for Well Dingye 2HF, 4627 m for Well Nanye 1HF, and 3297.96 m for Well Jinye 1HF). Formation temperature may be up to 145 °C. The length of horizontal section may reach 1034−1160 m. In accordance with previous reservoir evaluation, high-graded deep shale has an average permeability of 0.05−0.29 mD and average porosity of 2.92−5.81%; rock brittleness is 47−49% and the fracability index is 21−38%. As per well logging interpretation, the minimum stress is 105−109 MPa for Well Dingye 2HF and 100−107 MPa for Well Nanye 1HF; the difference between the maximum and minimum stresses is 23−28 MPa and 22−25 MPa, respectively. Horizontal stress difference is 12.3−17.3 MPa for Well Jinye 1HF. In view of the impacts of confining pressure and temperature which are not involved in a conventional stress−strain test, drill core burst tests for Well Dingye 2HF were conducted under different closure pressures and temperatures and the results are shown in Figs. 1 and 2. The stress−strain relationship of the drill core exhibits linear behavior under a low closure pressure and non-linear behavior under an increased closure pressure. At a low temperature, the shale core may be split instantly under the peak pressure to generate many cracks, whereas at a high temperature, the core exhibits sustained plastic deformation to generate shearing cracks before the peak pressure is reached. Therefore, non-linear deformation must be taken into account in the fracturing design for a deep shale gas well.

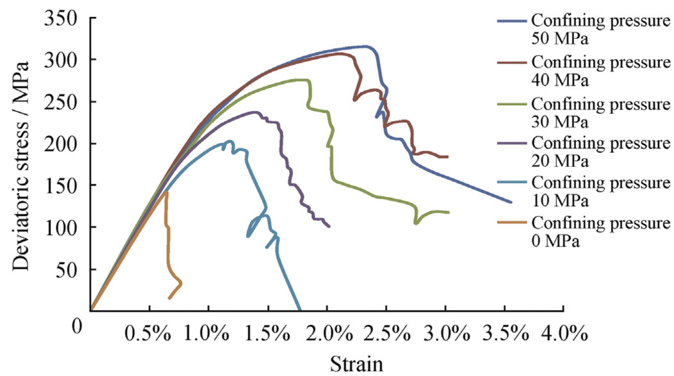

Fig. 1. Shale core stress−strain tests under different confining pressures.

2. Deep shale fracturing techniques

Deep shales buried at different depths and temperatures may have various brittleness, rock mechanical properties and stresses. Wellhead fracturing pressure is very high ranging in 95−115 MPa; the operating pressure may also reach 100 MPa. Some issues, such as how to predict fracturing pressure, lower operating pressure and improve flow conductivity and effective stimulated volume, should be addressed for the fracturing of deep horizontal shale gas wells [7−10]. This paper discussed the model of fracturing pressure and the methods of lowering operating pressure, increasing stimulated volume at high stress difference, improving flow conductivity under high closure pressure, and increasing proppant−fluid ratio and proposes a portfolio of techniques for deep horizontal shale gas well fracturing.

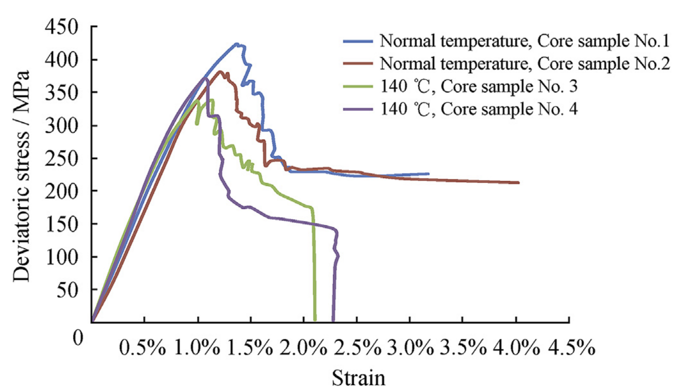

Fig. 2. Shale core stress−strain tests at different temperatures.

2.1. Fracturing pressure model

Fracturing pressure is crucial to the design and optimization of frac displacement, proppant−fluid ratio, intensity of well completion pipe string, power of fracturing trucks, frac wellhead, and surface pipe manifold. In view of high operating pressure for deep shale, many problems may be caused due to the inaccuracy in fracturing pressure prediction. For example, the displacement may be insufficient as per the design or the window of safety pressure may be too small to accomplish a frac operation. For predicting deep shale fracturing pressure accurately, the non-linear deformation at high temperature and high pressure must be taken into account.

2.1.1. Non-linear constitutive model

Duncan model, a non-linear elastic model established in terms of generalized Hooke's law, was employed to characterize the non-linear stress–strain behavior of deep shale. The model has 8 physical parameters which could be determined through static triaxial test. For any stress (σ_1, σ_3), the tangent modulus and Poisson's ratio would be calculated by Duncan equation.

$$E_t = Kp_a\left(\frac{\sigma_3}{p_a}\right)^n\left[1-\frac{R_f(\sigma_1-\sigma_3)(1-\sin\varphi)}{2c\cos\varphi+2\sigma_3\sin\varphi}\right]^2 \tag{1}$$

$$v_t = \frac{G-F\lg(\sigma_3/p_a)}{\left\{1-D(\sigma_1-\sigma_3)\Big/\left[Kp_a\left(\frac{\sigma_3}{p_a}\right)^n\left(1-\frac{R_f(1-\sin\varphi)}{2c\cos\varphi+2\sigma_3\sin\varphi}\right)^2\right]\right\}^2} \tag{2}$$

where, E_t is the tangent modulus in MPa; p_a is the barometric pressure in MPa; K, n, φ, c and R_f are the parameters of the material; σ_1 is the minimum principal stress in MPa; σ_3 is the confining pressure in MPa; v_t is the tangent Poisson's ratio; G, F and D are the constants of the test.

Here we take Well Dingye 2HF as an example. Eight parameters were fitted as K = 2957.3314, n = 0.8233, φ = 33.44°, c = 32.33 MPa, R_f = 0.8, G = −0.2559, F = 0.1832, and D = 69.058. The modulus E_t and Poisson's ratio v_t for (σ_1, σ_3) were then calculated by substituting these values into Eqs. (1) and (2). As is shown in Fig. 3, the shapes of the fitting curves by Duncan model are basically reconciled with the experimental curves; the strain deviation is mainly caused by horizontal cracks in the core samples collected from the bottom hole. In the compression test, the core samples will experience an axial strain to close the cracks before it is subject to axial pressure, which leads to the strain deviation.

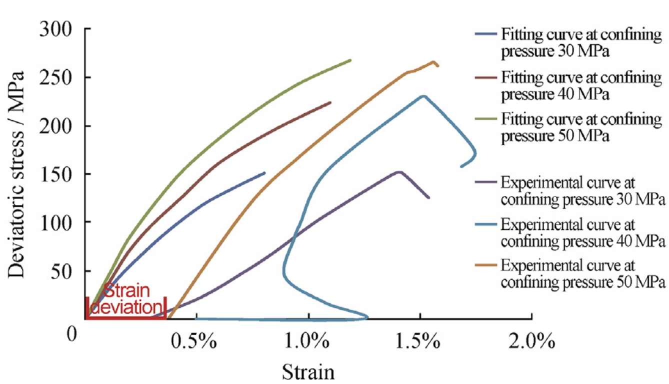

Fig. 3. Fitting curves by Duncan model and testing results.

2.1.2. Finite-element model for fracturing pressure prediction

A shale gas well would generally be completed with casing string first and then perforated. Rock burst is mainly caused by the fluid pressure directly acting on the rock inside the perforation and fluid column pressure conducted through the cement mantle from the casing pipe. In view of the transverse isotropy of shale and the infiltration process of fracturing fluid, a finite-element model was built to characterize the stress around the clustered perforations in a horizontal well. Some assumptions were made to improve computational efficiency and accuracy. (1) The fluids inside the perforations and wellbore are nearly static before rock burst, which means that even load on the borehole wall and perforation wall can be used to replace fluid column pressure. (2) The wellbore, cement mantle and formations are well cemented; therefore relative slip deformation is not involved in the model. (3) The impact of the infiltration process on fracturing pressure is involved. (4) Rock burst conforms to the principle of the maximum tensile stress. When the maximum tensile stress exceeds the tensile strength of the rock, the rock would be pulled apart to generate cracks.

The non-linear constitutive model of shale includes an elastic model and a plastic model. The former is set to be an anisotropic model and the latter an extended Drucker–Prager model. The process of dynamic pressurization from fracturing fluid injection is simulated by applying surface load of fracturing fluid pressure and pore pressure on the inner walls of the wellbore and perforations. The pressure of fracturing fluid increases with more and more fluid injected until the maximum principal stress reaches the tensile strength of the rock, when the rock is broken down and the pressure of fracturing fluid now is equal to the fracturing pressure. The hexahedral grid is employed and more grids would be created around the wellbore and perforation clusters to improve the computational accuracy.

The critical bottom-hole pressure for Well Dingye 2HF was calculated to be 125.20 MPa by the non-linear constitutive model, equivalent to the surface pump pressure of 97.18 MPa, which is 10 MPa more than the calculation by the linear elasticity model and is in good agreement with the actual fracturing pressure of 94 MPa. This constitutive model was verified to be credible.

2.2. How to lower operating pressure

High operating pressure resulting from large burial depth and pipeline frictional drag must be lowered for a safe fracturing operation. The methods include using a fracturing fluid system with low frictional drag, enlarging pressure window, and making in-situ adjustments [11].

2.2.1. Pretreatment with dilute mud acid

A preliminary treatment with hydrochloric acid is usually necessary for shale fracturing and may lower the fracturing pressure and operating pressure by 6.0 MPa. For a deep shale operation, another treatment with dilute mud acid composed of 15% HCl + 1.5% HF is utilized to significantly reduce the operating pressure. As per the field tests for Well Nanye 1HF, pressure drop may be 15 MPa on the average (Fig. 4).

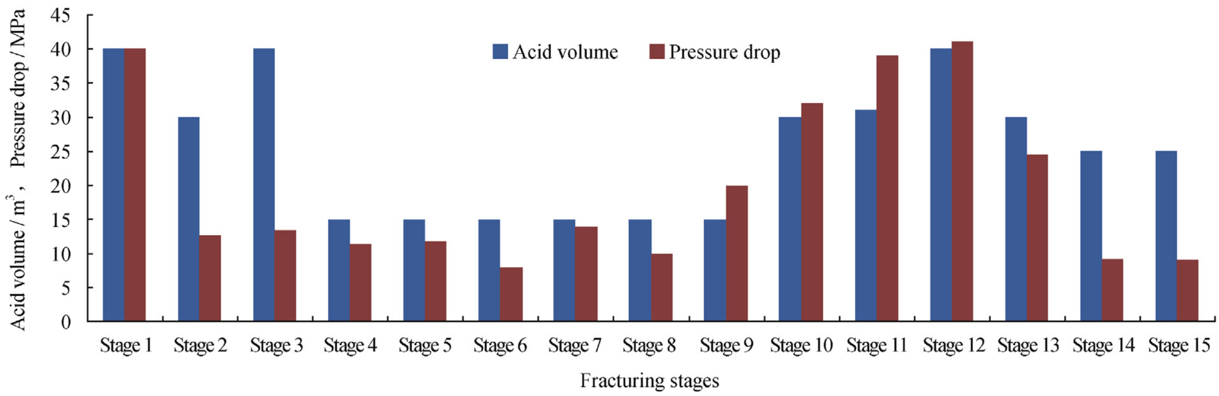

Fig. 4. Pretreatment with dilute mud acid and pressure drop in Well Nanye 1HF.

2.2.2. Perforating parameter optimization

The operating pressure would also be affected by the perforation friction, which is related to the displacement, perforation density and perforation diameter.

$$\Delta p_{\mathrm{pf}} = 2.33 \times 10^{-10} \frac{Q^2 \rho_{\mathrm{s}}}{(D_{\mathrm{en}} h)^2 D_{\mathrm{p}}^4 C_{\mathrm{p}}^2} \tag{3}$$

where, Δp_{pf} is the perforation friction, in MPa; Q is the displacement quantity, in m^3/min; ρ_{s} is the fluid density, in kg/m^3; D_{en} is the perforation density, in shot/m; h is the effective penetration, in m; D_{p} is the perforation diameter, in m; C_{p} is the discharge coefficient.

As per Eq. (3), the perforation friction is less dependent on perforation density for a small displacement and may increase greatly with the decreased perforation density for a large displacement. For a displacement of 12 m^3/min, the perforation friction is 21 MPa for the perforation density of 14 shots/m and decreases by 51% for the perforation density of 20 shots/m.

The perforation diameter has similar impacts. The perforation friction is less dependent on perforation diameter for a small displacement and may increase greatly with decreased perforation diameter for a large displacement. For a displacement of 12 m^3/min, the perforation friction would decrease by 8.3 MPa if the diameter increases from 10 mm to 12 mm; if the diameter exceeds 12 mm, the perforation friction will less decrease with the diameter (Fig. 5).

In terms of in-situ displacement, perforation friction dependence on perforation density and perforation diameter, and the performance of perforating gun and charge, the perforation density and diameter were optimized to be 20 shots/m and more than 12 mm, respectively; as a consequence, the perforation friction could decrease by more than 6 MPa compared with a conventional perforation.

2.3. Volumetric fracturing at high stress difference

Induced stress generated by artificial fractures may overcome the difference between the maximum and minimum principal stresses to turn the fractures or open natural fractures [12–14], which may create a complicated fracture network with a number of major fractures and intercrossed branches to realize a large stimulated volume. If the original earth stress is stacked with induced stress, the stress in the direction along the original maximum principal stress may be smaller than or equal to that in the direction along the original minimum principal stress, i.e. $\sigma_x - \sigma_y \geq \sigma_H - \sigma_h$; therefore, the branches may turn aside from the original direction and extend in parallel with the horizontal section and finally return to the original direction after propagating for a distance. As per the study, the net pressure of shale fracturing is usually less than 15 MPa and induced stress is also less than 15 MPa. For a reservoir with small stress difference, it is possible to veer the fractures or re-open those closed natural fractures. If the stress

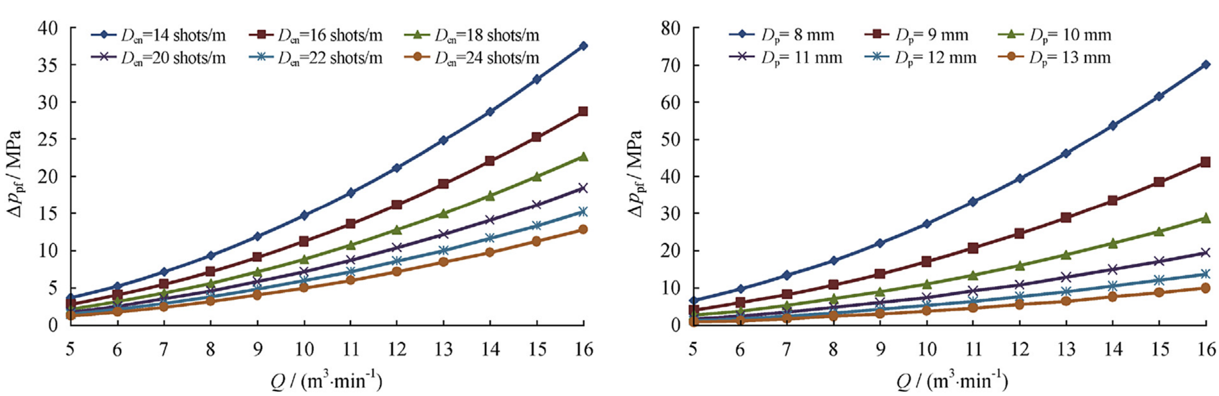

Fig. 5. Perforation friction dependence on perforation density and perforation diameter.

difference is large (>15 MPa), it is hard to induce a stress high enough to overcome the stress difference (Fig. 6). Therefore, the number of clusters and stimulated volume of deep shale should be optimized as per the requirements of increasing the number of fractures and decreasing the perforation friction; total displacement should be sufficient for single-shot displacement. For a perforation density of 20 shots/m and per-cluster penetration of 0.5 m, the number of clusters was estimated to be 5—6. In addition, the fractures may be blocked up temporarily to enlarge fracture opening.

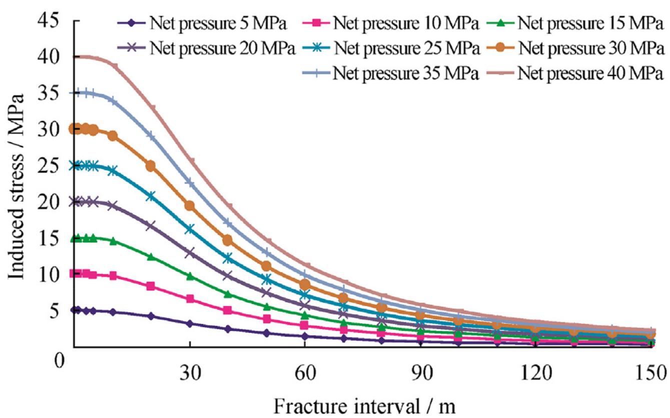

Fig. 6. Induced stress dependence on net pressure and fracture interval.

2.4. Enhancing flow conductivity under high closure pressure

Flow conductivity of fracture would affect post-frac production. The gradient of closure pressure for deep shale is about 0.023 MPa/m; for the burial depth of 3500—4500 m, the closure pressure may reach 80.5—103.5 MPa, which could not be sustained by ceramsite proppants of 70/140 mesh (Fig. 7). An alternative is to use a large amount of high-strength ceramsite of 40/70 mesh. Slug injection of proppants may also be feasible for the reservoir, e.g. Jiaoshiba shale, with relatively low closure pressure and complicated fracture network [15], because shearing cracks or a fracture network may be apt to preserve flow conductivity. For a deep shale with a relatively simple fracture network, the proppants added through slug injection is liable to break down and close the fractures; consequently flow conductivity would be deteriorated. It is suggested to inject the proppants uninterruptedly if possible. In summary, it is recommended to use the proppants with high flow conductivity which should be injected continuously to achieve high flow conductivity in the reservoir with high closure pressure.

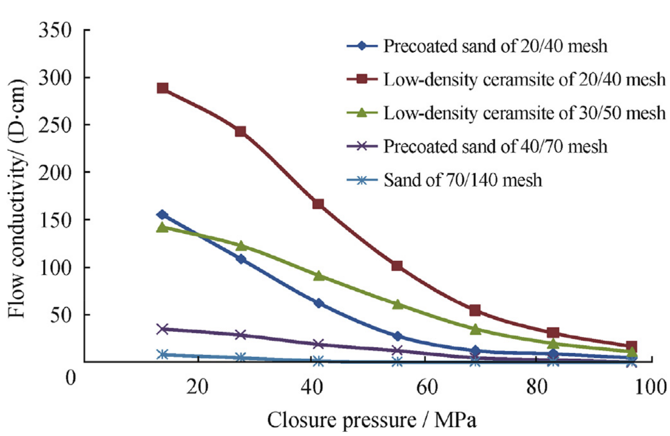

Fig. 7. Flow conductivity of proppants with different grain sizes under different closure pressures.

2.5. Improving proppant—fluid ratio

It is hard to improve proppant—fluid ratio by deep shale fracturing due to large burial depth and high minimum principal stress. The fractures would contract at high earth stress, making it difficult to admit more proppants [16]. It is inevitable to use a large displacement of viscous fracturing fluid to increase fracture width; but a high viscosity may inhibit the generation of a complicated fracture network and a large displacement may boost pipe friction and operating pressure. As per the study, fracture width may be increased by pad gelled fluid. If the viscosity is increased from 5 to 90 mPa·s, fracture width may be enlarged by 0.3 mm; if the volume of pad gelled fluid reaches 200 m^3, fracture width may be enlarged by 0.4 mm. A displacement exceeding 12 m^3/min would have less impact than the viscosity and fluid volume on fracture width. In summary, proppant—fluid ratio is much dependent on the viscosity of fracturing fluid and the volume of gelled fluid; therefore it is suggested to use gelled fluid + slick water + gelled fluid for deep shale fracturing.

3. Field tests and results

3.1. Field operation

The above techniques have been successfully applied to the fracturing of three wells. The operation is detailed as follows.

3.1.1. Dingye 2HF

The 12-stage fracturing operation began on October 16, 2013 with stage spacing of 60—120 m, 2 clusters in each stage, pretreatment by 15% HCl, displacement of 12—13 m^3/min, single-stage fluid injection of 1007—2780 m^3, total fluid injection of 29521 m^3, single-stage proppant injection of 22—34 m^3, total proppant injection of 319 m^3, average proppant concentration of 1.1%, proppants composed of ceramsite of 100 mesh and precoated ceramsite of 40/70 mesh, and operating pressure for slug injection of 85—95 MPa.

3.1.2. Nanye 1HF

The 15-stage fracturing operation began on March 23, 2014 with stage spacing of 64—99 m, 2 clusters in each stage, pretreatment by 15% HCl + 1.5% HF, displacement of 12—14 m^3/min, single-stage fluid injection of 2400—3600 m^3, total fluid injection of 46366 m^3, single-stage proppant injection of 28—73 m^3 with an average of 50 m^3, total proppant injection of 756 m^3, average proppant concentration of 1.6%, proppants composed of ceramsite of 100-mesh and precoated ceramsite of 40/70 mesh, and operating pressure for long-slug injection of 85–113 MPa.

3.1.3. Jinye 1HF

The 15-stage fracturing operation began on November 13, 2014 with stage spacing of 62–97 m, 2–3 clusters in each stage, pretreatment by 15% HCl, displacement of 10–18 m^3/min, total fluid injection of 26528 m^3, average single-stage fluid injection of 1768 m^3, total proppant injection of 1114 m^3, average single-stage proppant injection of 74 m^3, average proppant–fluid ratio of 4.2%, and operating pressure of 70–90 MPa.

3.2. Post-frac results

For Well Dingye 2HF, the initial production was 10.5×10^4 m^3/d; the initial stable production was 4.5×10^4 m^3/d; current gas output quickly declines to 2.3×10^4 m^3/d; current wellhead pressure is 8.1 MPa; daily fluid output is 30 m^3; cumulative fluid production is 8156 m^3; flowback rate is 26.4%. For Well Nanye 1HF, the initial production was 1200 m^3/d; by May 19, 2014, daily gas output was 800 m^3, casing pressure was 2 MPa, daily fluid output was 180 m^3, cumulative fluid production was 10419 m^3, and flowback rate was 22.5%. For Well Jinye 1HF, post-frac open flow was 10.5×10^4 m^3/d and stable gas yield was $(4.0–5.0) \times 10^4$ m^3/d; by April 15, 2015, stable production lasted more than 4 months and wellhead pressure was 22.1 MPa, indicating a good result of stable production. Production testing is being conducted now. As per post-frac results, geologic breakthrough has been made in Well Dingye 2HF and a commercial gas flow is expected to be yielded in Well Jinye 1HF.

3.3. Summaries

Deep shale fracturing and post-frac results could be summarized as follows.

1) Due to variable high operating pressure for deep shale fracturing, it is hard to improve proppant concentration and fluid injection.
2) Proppant–fluid ratio may be improved by using mixed fluids and high-viscosity fluid. With proper mixed fluids, the proppant–fluid ratio was increased from 1.1% for Well Dingye 2HF to 4.2% for Well Jinye 1HF.
3) It is hard to generate a complicated fracture network if the stress difference is large. For Wells Dingye 2HF and Nanye 1HF, the difference between the maximum and minimum principal stresses exceeds 20 MPa; *G* function shows that the fracture network is somewhat underdeveloped. On the contrary, Well Jinye IHF has been fractured with a complex fracture network.
4) Good reservoir properties are the prerequisite to a successful fracturing and production. High post-frac yield from Well Jinye 1HF is attributed to its high gas saturation, high brittleness and abundant bedding fissures.
5) High yield and stable production are greatly dependent on flow conductivity and stimulated volume, which may be improved by increasing fracturing fluid viscosity, sand injection volume, proppant–fluid ratio and the complexity of fracture network. For Well Jinye 1HF, the fluid with high viscosity accounted for more than 45% of total fluid injection; single-stage sand volume reached 74 m^3; the average proppant–fluid ratio reached 4.2%. This fracturing operation gave rise to a stimulated volume of 2900×10^4 m^3 and flow conductivity of 1.8–3.0 D·cm. Post-frac yield was stabilized at $(4.0–5.0) \times 10^4$ m^3/d.

4. Conclusions and suggestions

1) Deep shale usually exhibits non-linear deformation and fracturing behavior due to the large difference between the maximum and minimum principal stresses, which makes it difficult to generate a complex fracture system. For deep shale fracturing, target-oriented techniques different from those for the shale buried in shallower zones must be used.
2) A model for predicting the fracturing pressure of deep shale is established based on a non-linear constitutive model. The prediction is in good agreement with the actual fracturing pressure.
3) A safe fracturing operation for deep shale is greatly dependent on a lower operating pressure, which may be accomplished through the pretreatment with dilute mud acid, and by large-hole perforation and multi-slug injection.
4) Good reservoir properties are the prerequisite to the construction of high flow conductivity and stimulated volume. For deep shale fracturing, effective techniques include multi-cluster large-hole perforation, pad fracturing fluid with high viscosity, proppant with high flow conductivity and large-scale continuous proppant injection.
5) It is absolutely wrong to apply a fracturing technology uniformly to various deep shale gas prospects in China regardless of their different geologic conditions. Different reservoir properties should be tackled with target-oriented techniques including well completion, hydrofracturing, fracturing fluid, and volumetric fracturing.

References

[1] Wood DD, Schmit BE, Riggins L, Johnson BJ, Talley CA. Cana Woodford stimulation practices – a case history. In: North American Unconventional Gas Conference and Exhibition. Texas, USA: The Woodlands; 14–16 June 2011. http://dx.doi.org/10.2118/143960-MS.
[2] Fonseca E, Farinas MJ. Hydraulic fracturing simulation case study and post frac analysis in the Haynesville shale. In: SPE Hydraulic Fracturing

Technology Conference. Texas, USA: The Woodlands; 4−6 February 2013. http://dx.doi.org/10.2118/163847-MS.
[3] Guo Xiaozhe, Zhou Changsha. Diffusion seepage model for fractured horizontal well in shale gas reservoir. J Southwest Petroleum Univ Science Technol Ed 2015;37(3):38−44.
[4] Pope C, Peters B, Benton T, Palisch T. Haynesville shale − one operator's approach to well completions in this evolving play. In: SPE Annual Technical Conference and Exhibition; 4−7 October 2009. http://dx.doi.org/10.2118/125079-MS. New Orleans, Louisiana, USA.
[5] Dong Dazhong, Zou Caineng, Yang Hua, Wang Yuman, Li Xinjing, Chen Gengsheng, et al. Progress and prospects of shale gas exploration and development in China. Acta Pet Sin 2012;33(S1):107−14.
[6] Zhou Dehua, Jiao Fangzheng, Jia Changgui, Jiang Tingxue, Li Zhenxiang. Large-scale multi-stage hydraulic fracturing technology for shale gas horizontal well JY1HF. Pet Drill Tech 2014;42(1):75−80.
[7] Chen Zuo, Xue Chengjin, Jiang Tingxue, Qin Yuming. Proposals for the application of fracturing by stimulated reservoir volume (SRV) in shale gas wells in China. Nat Gas Ind 2011;30(10):30−2.
[8] Xiao Gang, Tang Ying. Shale gas and its exploration & development. Beijing: Higher Education Press; 2012.
[9] Duan Yonggang, Cao Tingkuan, Yang Xiaoying, Zhang Ying, Wu Guiping. Simulation of gas flow in nano-scale pores of shale gas deposits. J Southwest Petroleum Univ Sci Technol Ed 2015;37(3):63−8.
[10] Lin Lamei, Zhang Jinchuan, Tang Xuan, Jing Tieya, Zhu Liangliang. Conditions of continental shale gas accumulation in China. Nat Gas Ind 2013;33(1):35−40.
[11] Zhao Jinzhou, Li Zhiqiang, Hu Yongquan, Ren Lan. Numerical simulation of productivity after fracturing with consideration to micro-seepage in shale reservoirs. Nat Gas Ind 2015;35(6):53−8.
[12] Li Xin, Duan Shengkai, Sun Yang, Zhou Denghong, Sun Lei, Li Shilun. Advances in the exploration and development of U.S. shale gas. Nat Gas Ind 2011;31(8):124−6.
[13] Li Yongming, Xu Wenjun, Zhao Jinzhou, Dai Xiaolu, Wang Yanchen. Criteria for judging whether hydraulic fractures cross natural fractures in shale reservoirs. Nat Gas Ind 2015;35(7):49−54.
[14] Liu Dehua, Xiao Jialin, Guan Fujia. Current situation and research direction of shale gas development. J Oil Gas Technol 2011;33(1):119−23.
[15] Du Jinhu, Yang Hua, Xu Chunchun, Liang Shijun, Pi Xuejun, Wang Hongyan. A discussion on shale gas exploration and development in China. Nat Gas Ind 2011;31(5):6−8.
[16] Gao Shikui, Zhu Wenli, Yin Cheng. An economic analysis of shale gas resources: a case study of the Marcellus Shale Play. Nat Gas Ind 2014;34(6):141−8.